

By comparison with the absolute fluxes of the solar coronal lines which were measured when the sun was in a quiescent state we got the result that for 10 stars the upper limit of the scaling factors are between 2,000 and 8,000. We have got higher values for the other 4 stars because we have spectroscopic data only for the  $\lambda$  6375 line, the intensity of which in the sun is smaller by a factor of 4.5 compared to the  $\lambda$  5303 line. Since these results are for the quiet sun, we would get even lower values if we took the absolute solar line fluxes for a more active sun.

These results lead us to the conclusion that the intensity of any  $10^6$  K corona is less than 8,000 times that of the sun, while lines forming in  $10^4$  to  $10^5$  K gas are  $10^4$  to  $10^6$  times stronger than those of the sun. From this one may conclude that T Tauri stars in general do not have an extensive corona.

## Proceedings of the ESO Conference on “Scientific Importance of High Angular Resolution at Infrared and Optical Wavelengths” Now Available

The proceedings of this conference have just been published. The price for the 450-page volume is DM 50,- (including postage) and has to be prepaid.

Please send your order to:

European Southern Observatory  
Karl-Schwarzschild-Str. 2  
D-8046 Garching bei München  
Fed. Rep. of Germany

# Paschen and Balmer Lines in Active Galactic Nuclei

*K. J. Fricke and W. Kollatschny, Universitäts-Sternwarte Göttingen*

## 1. Introduction

If there is substantial disagreement between an observational result and its expectation from established theory, astronomers tend to speak of a “problem”. One of those problems which bothered optical and UV astronomers during the past years is the discrepancy of the observed ratio of the Ly $\alpha$  and H $\beta$  line intensities with the value of this ratio predicted by simple recombination theory for a photoionized hydrogen gas.

In this process, ionization electrons are recaptured into higher levels and excited atoms formed this way decay to successively lower levels by radiative transitions, finally reaching the ground level. Thereby the various hydrogen recombination spectra are emitted. The lowest of them are the Lyman, Balmer and Paschen spectra (cf. Fig. 1). Now, the Ly $\alpha$ /H $\beta$  ratio observed in quasars and active galactic nuclei are found to be by a factor of 3 to 10 times less than the theoretically predicted value ( $\sim 30$ ). There may be ways around the Ly $\alpha$ /H $\beta$  problem by modifying the simple theory, but the solutions are unfortunately not unique. Some theorists believe that special radiative transport effects in the spectral lines and electron collisions during the line-formation process cause enhanced Balmer line strengths and thereby depress the Ly $\alpha$ /H $\beta$  ratio. If the entire discrepancy is not to be explained by such processes alone, interstellar dust within and/or around the line-emitting regions (which are up to several light years across) may help to reconcile theory with observations (cf. e.g. Davidson, K. and Netzer, H., 1979, *Rev. Mod. Phys.*, Vol. 51, No. 4, p. 715). To explain this, we have plotted in Fig. 2 the standard interstellar extinction curve as a function of wavelength known from our Galaxy. Along the curve we indicated the locations of the various hydrogen lines. It is obvious that the influence of dust extinction on these lines must be quite different due to its strong wavelength dependence. It is also recognized that P $\alpha$  and P $\beta$  are relatively unaffected by dust as a result of the decrease (approximately  $\propto 1/\lambda$ ) of the extinction curve towards longer wavelengths. Moreover, because P $\alpha$  and H $\beta$  originate from the same upper atomic level, the P $\alpha$ /H $\beta$  ratio may be used as a sensitive indicator for the existence and importance of reddening by dust in addition to, or instead of, Balmer line enhancement due to optical depth effects. Therefore the measurement of the near infrared P $\alpha$  and P $\beta$  lines at 1.88 and 1.28  $\mu$ m,

respectively, may help to pin down an appropriate theoretical model for the hydrogen-emission-line region.

## 2. IR Spectrophotometry of P $\alpha$

As a result of strong efforts at various places (Caltech, ESO, La Jolla) on the technical side, the sensitivity and spectral resolution of infrared detectors has been substantially improv-

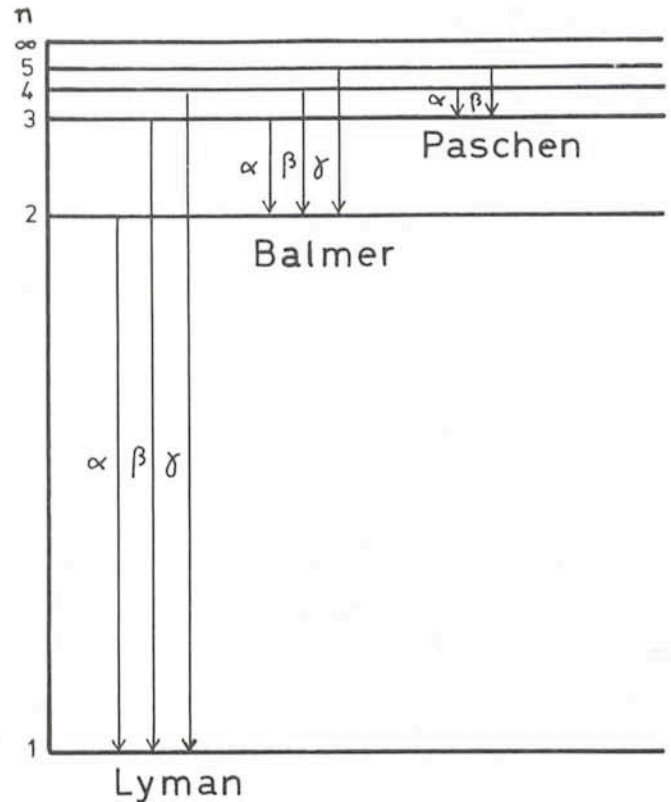


Fig. 1: Energy-level diagram for the hydrogen atom showing the Lyman, Balmer and Paschen series.  $n$  is the principal quantum number.

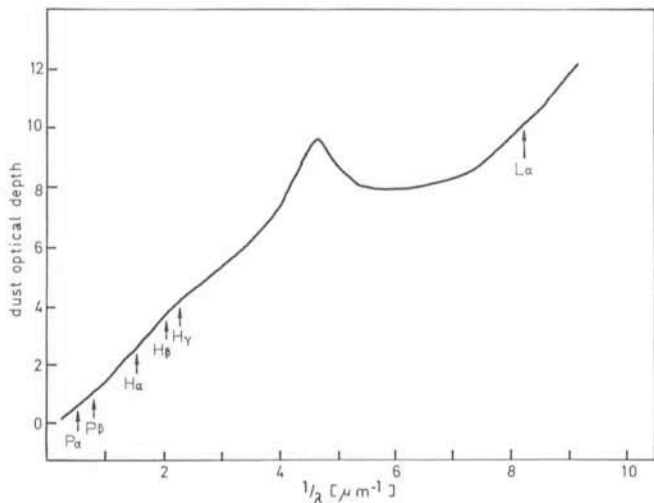


Fig. 2: Interstellar extinction curve for our Galaxy, as a function of reciprocal wavelength and with an arbitrary normalization. The wavelength positions of the main hydrogen lines in the infrared, optical and ultraviolet spectral ranges are indicated.

ed in order to make possible the spectrophotometry of IR lines in distant galaxies and quasars. Since 1980, with the beginning of period 26 at ESO, an InSb detector equipped with broad-band filters for photometry (1–5  $\mu\text{m}$ ) and with circular variable filters (CVF's) for narrow-band spectrophotometry (1.5–5.5  $\mu\text{m}$ ) became available at the ESO 3.6 m telescope (for details see the User's Manual by A. Moorwood and P. Salinari). The resolving power  $\lambda/\Delta\lambda$  of the CVF's ranges from 50 to 70. We were the first visiting astronomers at ESO who used this equipment. We applied it to measurements of the  $P\alpha$ -line strengths in active galactic nuclei.

The number of objects for which the Paschen lines are observable is strongly limited due to selective atmospheric extinction at IR wavelengths by the  $\text{H}_2\text{O}$  and  $\text{CO}_2$  molecules and for reasons of detector sensitivity as well as limiting apparent brightness of the sources themselves. In Fig. 3 the atmospheric transmission is plotted between 0 and 6  $\mu\text{m}$ . The

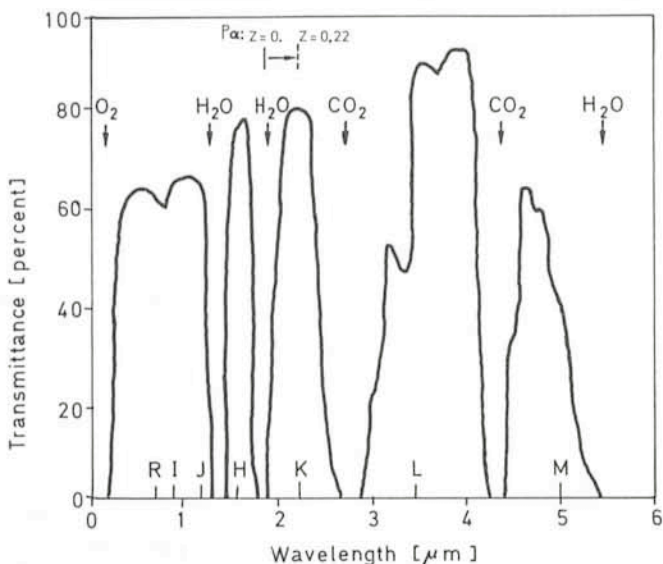


Fig. 3: The atmospheric transmission curve in the near and middle infrared as a function of wavelength. The infrared photometric bands are denoted by capital letters. The main absorbing molecules  $\text{O}_2$ ,  $\text{H}_2\text{O}$  and  $\text{CO}_2$  are responsible for the deep transmission gaps. The positions of an unshifted and a redshifted  $P\alpha$  line are also indicated.

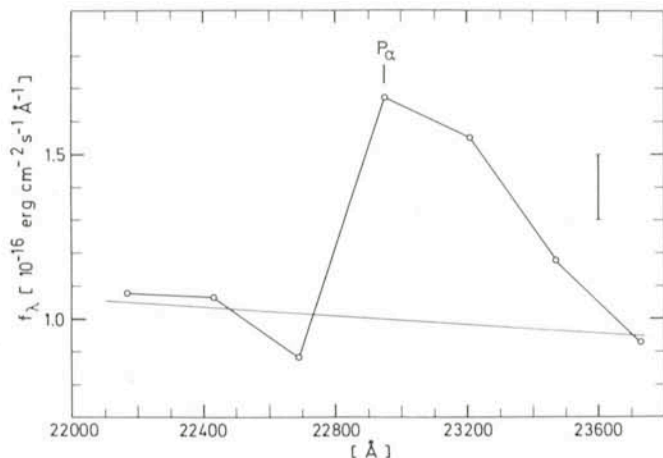


Fig. 4: The  $P\alpha$  line of the quasar PKS 0312-77 as measured with the InSb detector together with a circular variable filter at the ESO 3.6 m telescope.

rest wavelength of  $P\alpha$  falls right into an opaque band of our atmosphere. However, for the redshift range  $0.07 < z < 0.33$  of the sources the frequency of the  $P\alpha$  line is appropriately tuned in order to become observable in the adjacent frequency band, in which our atmosphere is much more transparent.

The location of the redshifted  $P\alpha$  line is indicated in Fig. 3 for the object PKS 0312-77. If both  $P\alpha$  and  $P\beta$  are to be observed simultaneously in the spectrum, the admissible redshift range is even smaller,  $0.23 < z < 0.33$ . Taking also into account the requirements of maximum exposure time and of visibility from La Silla, only 11 objects remain for  $P\alpha$  and  $P\beta$  observations out of the  $\sim 2,000$  objects contained in the lists of active nuclei and quasars (cf. e.g. M. P. Véron, P. Véron, 1974, "A Catalogue of Extragalactic Radio Source Identifications", *Astronomy and Astrophysics Supplement*, **18**, 309; A. Hewitt and G. R. Burbidge, 1980, "A Revised Optical Catalogue of Quasistellar Objects", *Astrophysical Journal, Supplement*, **43**, 57).

### 3. Results and Discussion

In our first run with the IR spectrophotometer at the ESO 3.6 m telescope in October 1980 we obtained  $P\alpha$  data for two objects: PKS 0312-77 and 3C 109. The first is a quasar with  $z =$

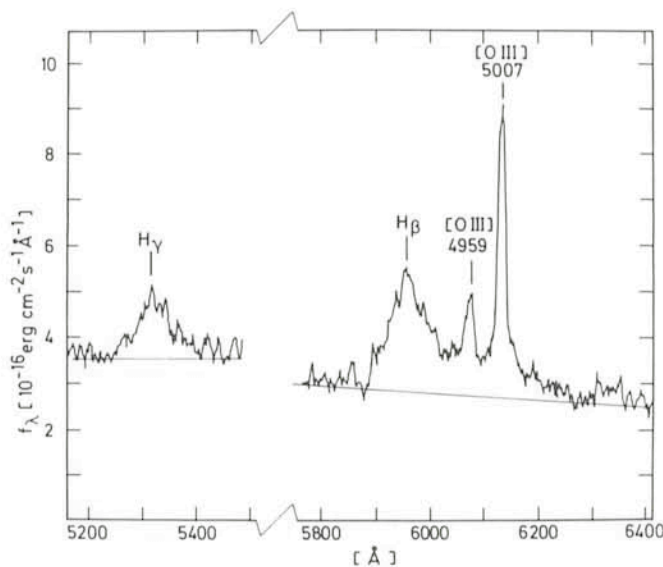


Fig. 5: Line profiles of  $H\gamma$  and  $H\beta$  for the quasar PKS 0312-77 as obtained with the image dissector scanner at ESO's 3.6 m telescope.

0.223, the latter a N galaxy having  $z = 0.306$ . We measured the profile at 7 equidistant wavelength positions symmetric around the expected line centre. We show in Fig. 4 the profile of the  $P\alpha$  line of the quasar; an estimated error bar is indicated. The accuracy of the profile compares favourably with  $P\alpha$  profiles obtained for some other objects by two American groups (Puetter et al., 1981, *Astrophys. J.*, **243**, 345; Soifer et al., 1981, *Astrophys. J.*, **243**, 369). During the same run we obtained Balmer line profiles with the Image Dissector Scanner attached to the Boller and Chivens spectrograph of the 3.6 m telescope. These are depicted for the same object in Fig. 5. The expected  $P\alpha/H\beta$  ratio from unmodified recombination theory is 0.35 (where a temperature of 10,000 K and opaque conditions are assumed). In our two objects we find comparatively enhanced values:  $1.24 \pm 0.3$  for the quasar and  $0.73 \pm 0.4$  for the galaxy. They are also higher than those found by Puetter and Soifer 1981 who find a range for this ratio from 0.09 to 0.72 for their sources with the exception of PG 0026+129, for which Puetter et al. found the very high ratio of 1.4 in 1978 (R. C. Puetter et al., 1978, *Astrophys. J., Lett.*, **226**, L53). The deviation from the recombination value may be explained by reddening in the sources and/or by optical depth effects. However, we think that the high  $P\alpha/H\beta$  ratios found by us indicate that the emission-line regions in nuclei are still poorly understood and substantial improvements in the line transfer calculations with and without dust absorption are necessary. Attempts in this direction are presently being done among others by R. C. Canfield and R. C. Puetter and by Mme S. Collin-Souffrin and collaborators.

Our observational results reported here are the subject of a more detailed paper (W. Kollatschny and K. Fricke, 1981, *Astron. Astrophys.*, in press). We are presently continuing our hydrogen-line observations in the infrared and optical spectral ranges using the ESO equipment and in the UV with the IUE

ANNOUNCEMENT OF AN ESO WORKSHOP ON

## The Most Massive Stars

ESO Munich, 23–25 November 1981

Among topics to be discussed in the workshop are the theory of evolution of massive stars, observations of luminous stars in the Galaxy and nearby systems, the effect of the presence of these stars on the structure and evolution of the interstellar matter in galaxies and their use as distance indicators.

The workshop will include both review papers and short contributions with ample time for discussion.

Contact address:

S. D'Odorico,  
Workshop on Massive Stars,  
ESO  
Karl-Schwarzschild-Str. 2  
D-8046 Garching bei München

satellite telescope in order to obtain complete sets of Lyman, Balmer and Paschen ratios for a sample of active galactic nuclei. We thus hope to provide useful constraints to improve the theoretical descriptions.

### Acknowledgement

This work was in part made possible by a grant (Fr 325/12 and Fr 325/15-2) of the Deutsche Forschungsgemeinschaft.

## UBV Photometry of Quasars

G. Adam, Observatoire de Lyon

### I. The Disappointed Hopes

#### 1. Hubble and the Birth of Observational Cosmology

Between the two world wars, a few people were, surprisingly, still concerned by extraterrestrial problems. One of them was Edwin Hubble, who discovered the so-called expansion of the universe, after proving the extragalactic nature of the great nearby spiral galaxies. Since then, astronomers have tried to understand the large-scale geometry of that newly opened universe. It is a long and still unsuccessful story. . .

How can we use the extragalactic objects to study that large-scale structure? There are two powerful methods:

(a) Counts of distant objects, up to some limiting magnitude. The dependence of the number of objects found on the radius sampled in the universe can in principle tell us if our universe is spherical and closed, or euclidean, or hyperbolic and open (a euclidean universe is just the kind of universe we like, with non-crossing parallels and circle area obeying the good old  $r$ -square law). In fact, the deceleration parameter  $q$  is the crucial one which defines the overall geometry.

(b) Plots of the recession velocity – or of the redshift  $z$  – of distant objects as a function of their measured luminosity. If we assume that the different objects have the same intrinsic luminosity, this is equivalent to a plot of the recession velocity versus the distance. Usually, one constructs a plot of  $\log z$

versus the apparent magnitude. For large values of  $z$ , the curves are very  $q$ -dependent and should tell us what is the "observational value", the one which fits best the experimental curves.

In fact, that approach initially failed: the most distant galaxies which can be observed are still too near to us, with  $z$  around 0.5. This is far too short an interval to allow a  $q$  determination.

#### 2. Quasars: The Cosmological Boom

In the early sixties, a new class of extragalactic objects entered the astronomical scene: the quasi-stellar objects, or quasars. Now, we have at hand lists of such objects which should soon reach the 2,000 entries, with large redshifts up to 3.53, and a lot of photometric measurements, mainly UBV. So it seems that solving the cosmological problem is just a matter of drawing a large Hubble diagram, fit a curve to the observational points, and write  $q$  in golden letters in the Great Book of Astronomical Achievements. But Figure 1, which is a Hubble diagram tying the B magnitude to the redshift for 358 quasars, has a most unpleasant look. . . The accuracy of modern UBV photometry is too high to account for such a scatter. In fact, there are three main difficulties:

(a) Use of the Hubble diagram assumes that all the objects observed have the same intrinsic luminosity. Unfortunately, this is very far from truth for quasars: at the same redshift, the